Iraqi Journal of Physics, 2026
https://doi.org/10.30723/ijp.v24i1.1503

Vol.24, No.1, PP. 43-54
P-ISSN: 2070-4003
E-ISSN: 2664-5548

Synthesis and Characterization of PPy:PEO Blend Dopant with $AgNO_3$ Nanoparticles: Optical and Electrical Investigations

Marwan M. Fadil[1] and Mohammed G. Hammed[1*]
[1]*Department of Physics, College of Science, University of Anbar, Ramadi, Iraq*
[*]*Corresponding author: Sc.moh72_gh@uoanbar.edu.iq*

Abstract
Nanocomposite films, based on polypyrrole (PPy) and polyethylene oxide (PEO), which can be doped with silver nitrate ($AgNO_3$) nanoparticles, were synthesized using pyrolysis spray technique at room temperature. The systematic study of optical and electrical properties of the prepared films was performed depending on dopant concentration (0, 3, 6, 9 and 12 wt. %). At about 400 nm, the UV-Vis spectrometer exhibits a noticeable absorption peak. Higher concentrations of $AgNO_3$ intensify the peak, especially in the sample containing 12% $AgNO_3$. Hall measurements were used to establish the type, concentration of charge carriers, and Hall mobility (μ_H). The results showed that the nanocomposite films had a negative Hall coefficient (n-type) prior to the addition of $AgNO_3$ nanoparticles. The polymer mix films exhibit (p-type) conductivity with a positive Hall coefficient at all $AgNO_3$ nanoparticle concentrations. In D.C. studies, electrical resistance decreases as temperature rises, but the nanocomposite film's D.C. conductivity rises as $AgNO_3$ nanoparticle concentrations rise. Across all produced samples, alternating electrical conductivity ($\sigma_{a.c}$) increases as frequency increases. At low frequencies, the alternating electrical conductivity doesn't change.

Article Info.

Keywords:
Silver Nitrate Nanoparticles, PPy:PEO Blend, Optical Properties, Hall Effect, Electrical Conductivity.

Article history:
Received: Jul. 14,2025
Revised: Oct. 04, 2025
Accepted:Oct. 30, 2025
Published:Mar.01,2026

1. Introduction
Polymers have gained a lot of interest in both the industrial and scientific sectors due to their distinctive chemical and physical characteristics, which make them essential parts of a wide range of technological applications [1, 2]. Their electrical conductivity, mechanical strength, optical efficiency, and thermal stability are all significantly influenced by their molecular structure and synthesis conditions. In recent years, a lot of attention has been paid to the optical properties of polymer composites, especially for the production of photoelectric and energy storage devices such light-emitting displays, organic solar cells, and supercapacitors [3]. Polymer nanocomposites stand out in this setting, since they combine the optical and electrical advantages of inorganic materials with the flexibility and processability of polymers. These composites improve qualities including light absorption, transparency, and refractive index, which makes them ideal for cutting-edge optical and electronic systems [4].

Conducting polymers (CPs) have garnered significant interest in materials research in recent decades due to their unique mix of metal-like electrical properties. One of the numerous CPs, polypyrrole (PPy), has garnered a lot of attention because to its ease of synthesis, high conductivity, exceptional environmental stability, and biocompatibility. Because of these characteristics, PPy is a viable option for a variety of applications, such as biomedical sensors, electronics, optical devices, actuators, antistatic coatings, and medical devices [5, 6]. However, pure PPy's intrinsic brittleness and poor solubility in common solvents frequently restrict its processability and usefulness [7, 8]. Combining PPy with other polymers has emerged as an acceptable way to overcome these difficulties. since of its hydrophilic nature and semi-crystalline structure, poly(ethylene oxide) (PEO) is an excellent selection for these blends because the material has high

solubility in water and organic solvents as well as notable thermal and chemical stability [9, 10]. The stiffness of PPy can be offset by PEO's flexibility and film-forming properties to create a composite material with better mechanical and processability properties. Combining these two polymers can result in a synergistic approach to creating new functional materials [4, 11]. It is a preferred choice for polymer electrolytes and optoelectronic devices due to its exceptional ionic conductivity in the amorphous state and compatibility with metal ions. Nevertheless, restrictions like a broad bandgap and low ionic conductivity continue to be problems, which motivate continuous attempts to improve its qualities by adding other additives, such as plasticizers and nanoparticles [12].

Moreover, dopants can be added to polymer mixtures to alter their intrinsic optical and electrical characteristics. This doping process greatly improves the conductivity of the polymer structure by introducing charge carriers. Metallic nanoparticles have shown themselves to be very successful dopants in this situation. Silver nitrate ($AgNO_3$) is added to polymer matrices to further improve their functionality [13, 14]. Because of their unique optical characteristics and exceptional electrical conductivity, which are ascribed to the localized surface plasmon resonance (LSPR), silver nanoparticles (Ag NPs) have attracted a lot of attention. Ag NPs can dramatically alter the material's electrical and optical properties when incorporated into a polymer matrix, opening the door for novel applications [15, 16].

The primary objectives of this study were to create and examine a PPy:PEO blend doped with $AgNO_3$ nanoparticles. The main objective was to comprehend how the addition of $AgNO_3$ nanoparticles to the PPy:PEO matrix affected the blend's optical and electrical characteristics. By carefully examining these characteristics, our study aims to provide significant insight into the structure-property correlations of these complex nanocomposite materials, potentially paving the way for their application in optoelectronic devices and other cutting-edge technologies.

2. Experimental Work

In order to create consistent and superior hybrid nanocomposite films, a number of meticulously regulated procedures were used in this work to prepare glass substrates, polymer dispersions, and nanomaterials. First, 1 mm thick glass slides were cut to 2.5 × 2.5 cm in order to be used as substrates for the deposition of PPy:PEO films containing $AgNO_3$ at different concentrations. To get rid of dust, oil, and other surface contaminants, the slides were carefully washed with soap and water. To further enhance surface cleanliness, this cleaning procedure was repeated with pure alcohol rather than distilled water. To avoid scratches and maintain a smooth surface, the slides were dried in a single vertical orientation after cleaning. Polymer solutions were created once the substrate was prepared. To guarantee a uniform dispersion, 0.1 g of PPy was dissolved in 100 mL of distilled water and magnetically agitated for two hours at 60°C. Similarly, to create a homogenous solution, 1 g of PEO was dissolved in 100 mL of distilled water and swirled under the same circumstances. 2.5 g of $AgNO_3$ were dissolved in 100 mL of distilled water to create the $AgNO_3$ solution. To guarantee efficient dispersion of the nanoparticles, the mixture was vigorously agitated for two hours at 27 °C using a high-speed magnetic stirrer.

Once the individual solutions were ready, a 50:50 blend of PPy and PEO was prepared by combining equal volumes of each solution and stirring them at 27 °C for 20 minutes to form a homogeneous polymer blend matrix. Various concentrations of $AgNO_3$ nanoparticles (0, 3, 6, 9, and 12%) were then added to the polymer blend, and each formulation was stirred for an additional 60 minutes to ensure proper mixing and nanoparticle dispersion. These final mixtures were subsequently used to fabricate

nanocomposite films by a pyrolysis spray technique, which was employed to produce nanocomposite films from a blend of PPy and PEO, including varying proportions of $AgNO_3$ nanoparticles. The solutions were atomized following redispersion with an ultrasonicator, with each deposition procedure lasting 60 minutes at 90 °C, incorporating intermittent spraying for 5 seconds and pauses of 15 seconds. Subsequently, the slides were covered in glass to avert contamination and were left in the laboratory. To guarantee complete drying and obtain homogeneous nanocomposite films. The mean thickness of the created thin film was 1584 nm.

Table1: Chemical substances and their origins.

Polypyrrole	
Chemical formula	$[C_4H_5N]_n$
Appearance	Black powder
Molecular weight (g/mole)	67.09
Company	AlFA-Chemistry
polyethylene Oxide	
Chemical formula	$H-[O-CH_2-CH_2]-O$
Appearance	Wight powder
Molecular weight (g/mole)	10000×(300)
Purity	98%
Company	CDM-Chemistry
Silver Nitrate	
Chemical formula	$AgNO_3$
Appearance	Colorless to white crystals
Molecular weight (g/mole)	169.873
Purity	99%
Company	Merck

3. Results and Discussion

3.1. X-Ray Diffraction (XRD) Analysis

The XRD patterns of PPy:PEO blended and PPy:PEO/$AgNO_3$ nanocomposite films with different in dopant concentrations are shown in Fig. 1. For the pure PPy:PEO blend, there is a broad peak at ∼2θ = 18.85° (the most intense) and a second less intense peak at ≈23°, indicating that polymer matrix is partially crystalline, while PPy has low crystallinity. A low intensity peak at 26.5°, related to structural ordering in the polymer backbone, is also detected.

The XRD pattern of PPY: PEO after composing with 3% $AgNO_3$ reveals new complementary peaks at 19.01°, 23.24°, 27.62°, 32.10°, 38.07°, 44.46°, and 46.4356°. The peak of diffraction of polypyrrole was seen with a 2θ value of 19.1°. Regarding polypyrrole in the scientific literature. It is noted that the diffraction peak is at 2θ ≈ 23.24°. This peak also appeared at concentrations 6, 9, and 12% of $AgNO_3$, which is identical to reported values for PPy (JCPDS No. 00-001-1041). PPy also shows a broad diffraction peak at about 2θ ≈ 27.62°. It displays the diffraction peaks at Bragg angles of 2θ ≈ 32.10°, corresponding to the crystallite plane (-111), which was following the JCPDS No. 01-084-1547. The diffraction peak is observed at 2θ ≈ 38.07° corresponding to the crystallite plane (011). The peak of diffraction is detected at 2θ ≈ 44.46° corresponding to the crystallite plane (012). This peak also appeared at concentrations 6, 9, and 12% of $AgNO_3$, which was following the JCPDS No. 00-043-1038. In addition, the peak of diffract is observed at 2θ ≈ 46.435° corresponding to the crystallite plane (211). This peak also

appeared at concentrations 12% of $AgNO_3$, which was following the JCPDS No. 01-076-1393.

The XRD pattern of PPy:PEO blend after composing with 6wt.% $AgNO_3$ shows new peaks at 23.82°, 31.65°, 38.02°, and 44.20°. The diffraction peak appears at $2\theta \approx 31.65°$, corresponding to the (- 111) crystallite plane, which matches JCPDS No. 01-084-1547. The XRD pattern of the PPy:PEO blend after adding 9% $AgNO_3$ shows new peaks at 12.59° and 20.46°, while PEO also shows a peak at approximately $2\theta \approx 20.4624°$, indicating the semi-crystalline nature of the polymer. Based on standard card No. 01-084-1547, a new peak at $2\theta = 31.6352°$ in Fig. 1 matches the (-111) crystallite Silver oxides were formed by mixing $AgNO_3$ into a blend of the conducting polymers PPy and PEO.</sent $AgNO_3$ was used to make Ag^+ ions, which were partially converted into metallic silver nanoparticles by the structure of polypyrrole Later, when exposed to oxygen in the solution or during the process, the metallic silver formed silver oxides, such as Ag_2O and AgO, via known oxidation reactions. By coordinating its ether oxygen atoms to Ag^+ ions, the PEO component stabilized the mixture, ensuring uniform dispersion of silver species and preventing agglomeration. As a result, a consistent PPy/PEO/AgO nanocomposite was created, with the silver oxides spread evenly in the polymer, giving it special optical and electrical features. This method for preparing silver oxide from $AgNO_3$ in polymer matrices aligns with previous studies on Ag–polymer mixtures [17, 18]. However, the peaks in the diffraction pattern are observed at angles of about 64.39° and 77.22°, which correspond to specific reference numbers and relate to certain crystal structures. These peaks were also observed at 12 wt.% $AgNO_3$ concentrations. Crystallite size was estimated using Scherrer's equation, whereas interplanar spacing was calculated based on Bragg's law. The results indicate that as the amount of $AgNO_3$ increased, crystallinity increased, and the sample with 12 wt.% had the highest crystallinity, indicating a better structure and less strain. All these results show that adding $AgNO_3$ changes the structure of the PPy:PEO matrix, making it more organised and creating a nanocomposite phase that can be used in optoelectronic or sensing applications.

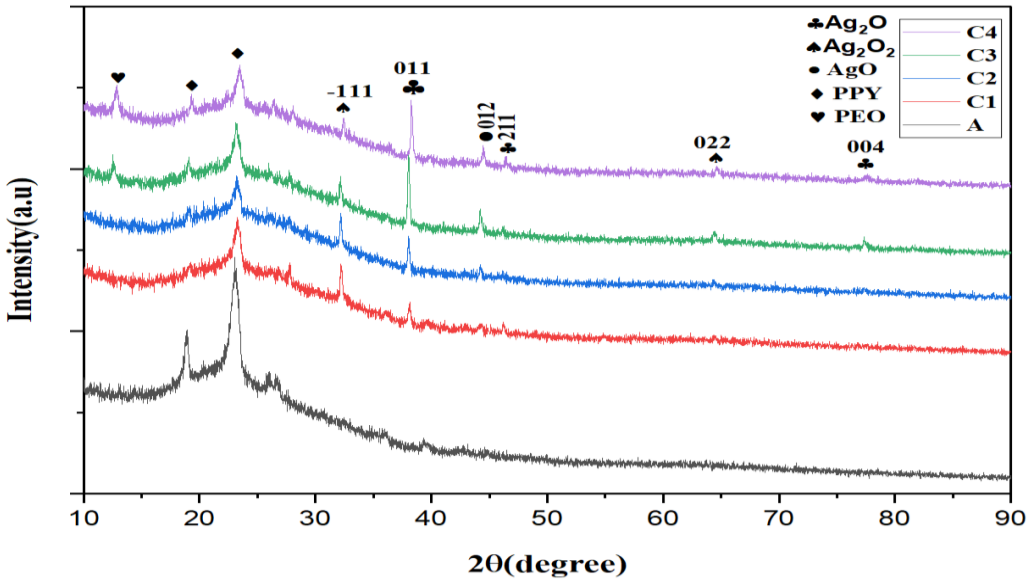

Figure 1: XRD of polymeric nanocomposite films after adding $AgNO_3$: (A) 0%, (C_1) 3%, (C_2) 6%, (C_3) 9% and (C_4)12%.

3.2. Optical Properties

- Absorbance (A)

UV-Visible, or ultraviolet-visible by examining how materials interact with electromagnetic radiation in the visible and ultraviolet spectrums, spectroscopy is a potent tool for characterizing materials, particularly polymers and nanocomposites. When several materials are mixed to create new nanocomposite films, this method offers important insights into the material's electronic structure, electronic transitions, and changes in these characteristics. With a minor rise in absorbance in the ultraviolet area (below 400 nm), the base blend's curve in Fig. 2 (black line) displays relatively low absorbance across the visible and near-infrared range (about 400–1100 nm). The π-π* electronic transitions in the aromatic pyrrole rings of the PPy backbone are mainly responsible for this band. Given that PEO absorbs poorly in this range, this behavior is expected [19], while PPy contributes higher absorbance, especially in the visible region [20]. transparent in this range.

A strong absorption peak at about 400 nm, and this peak gets stronger as the amount of silver nitrate increases, especially in the sample with 12% $AgNO_3$. This effect is particularly prominent in the UV region. With an increase addition of $AgNO_3$, a new absorption peak begins to emerge as a "shoulder" in the wavelength range of 400-500 nm. This peak is characteristic of the Surface Plasmon Resonance of Ag NPs formed within the polymer matrix. This formation occurs due to the reduction of silver ions (Ag^+) by the polymer blend components, especially PPy. This behavior occur which happens when free electrons on process results in significant light absorption at specific wavelengths, typically between 390 and 420 nm for Ag NPs. The absorption is significantly affected by particle size, buffer media, and chemical environment. As the concentration of $AgNO_3$ increases, the stronger absorption peak shows that more Ag NPs are being made in the prepared nanocomposite films, which leads to more plasmon resonance sites. The increase in absorbance intensity with higher $AgNO_3$ content indicates a greater number of silver nanoparticles being formed within the blend. This observation is consistent with the ٥absorbing species [22]. A slight change in the peak position or shape may indicate a difference in the size of the nanoparticles or how they clump together [23]. On the other hand, samples with lower amounts of $AgNO_3$ show a weak or unclear absorption peak, suggesting that there aren't enough nanoparticles produced to create a strong plasmonic response.

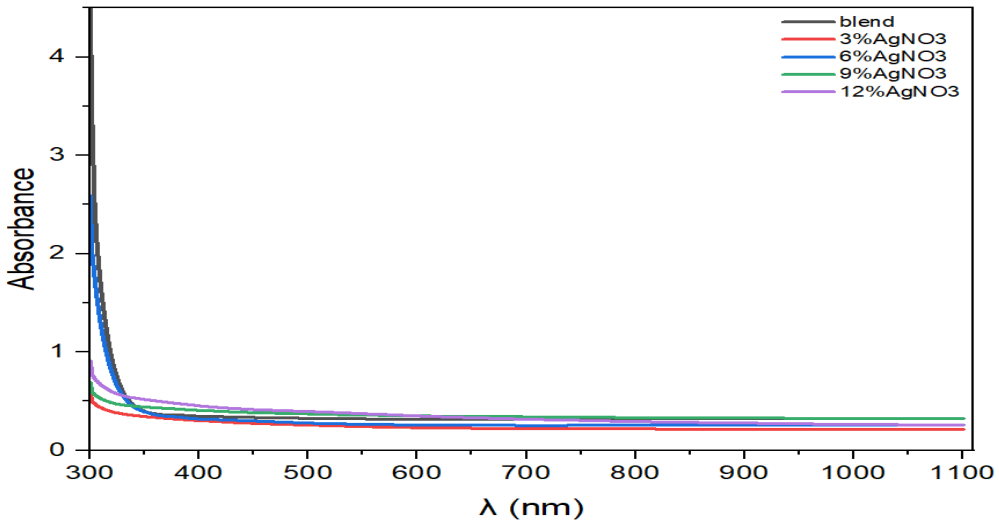

Figure 2: UV-VIS absorbance of PPy:PEO blend and their nanocomposite films with varying amounts of $AgNO_3$ (3, 6, 9 and 12 wt.%).

- **Transmission (T_r)**

The optical transmittance spectra of the PPy:PEO blend and its nanocomposite films doped with different concentrations of $AgNO_3$ are shown in Fig. 3. The pure polymer blend shows a moderate transmittance in the range of 0.45–0.50, suggesting that the matrix is not fully transparent. A gradual decrease of the optical transmittance over the entire given wavelength range can be noticed with increasing $AgNO_3$ concentration. This is because of the enhancement of light absorption and scattering by Ag NPs due to LSPR effect especially at length wavelengths. At a low dopant value (3 wt.%), more light passes through the nanocomposite film due to the fact that nanoparticles are uniformly dispersed in a polymer. However, at higher concentrations (6–12 wt.%) low transmittance (≤4%) and further reductions in transmittance are observed for even lower transmitted %T values. These results are in agreement with prior investigations in which the optical transmittance of polymer nanocomposites was strongly correlated with nanoparticle concentration, film thickness and structural homogeneity [24, 25].

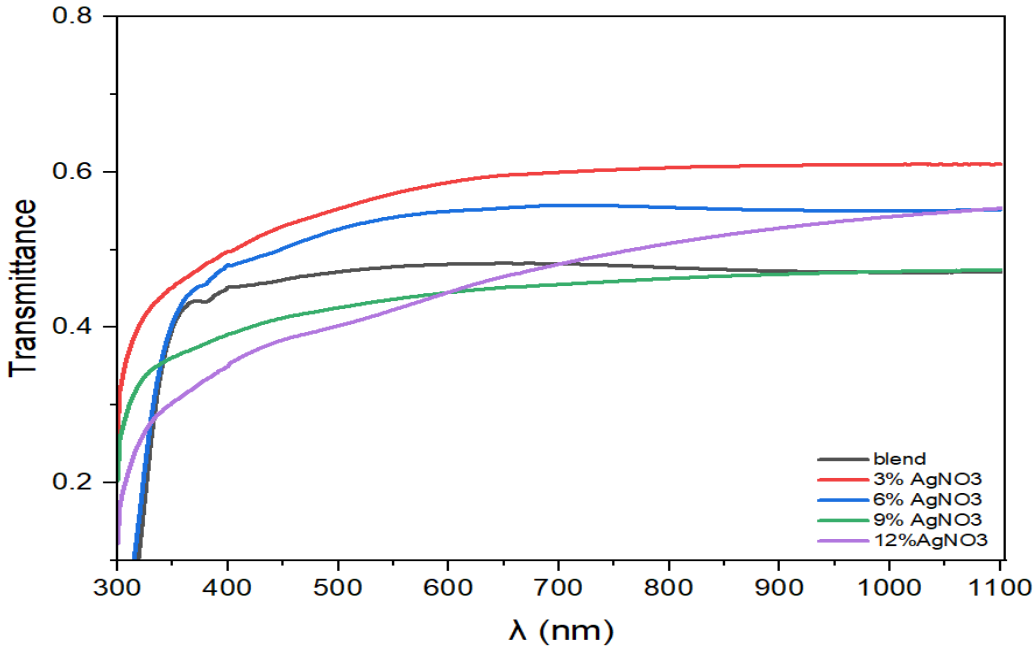

Figure 3: Transmission of PPy:PEO blends and their nanocomposite films with varying amounts of $AgNO_3$ (3, 6, 9 and 12 wt.%).

- **Refractive Index (n)**

Fig. 4 shows the relationship between the refractive index and wavelength for samples of the polymer blend reinforced with different percentages of $AgNO_3$. It is observed that the refractive index of all nanocomposite films is high at short wavelengths (300–400 nm) and gradually decreases with increasing wavelength, a typical behavior for insulating or semiconducting materials due to reduced electron scattering with increasing light energy. The data show that adding $AgNO_3$ greatly affects the optical properties: the refractive index decreases at a 3% weight concentration compared to the polymer blend film, but it slowly increases at higher concentrations (9 and 12% weight). This change occurs because Ag NPs form within the polymer blend, boosting SPR and altering the material's response to light. These results confirm that controlling the amount of $AgNO_3$

used and its placement is important for altering the optical properties of nano-supported polymeric materials [28].

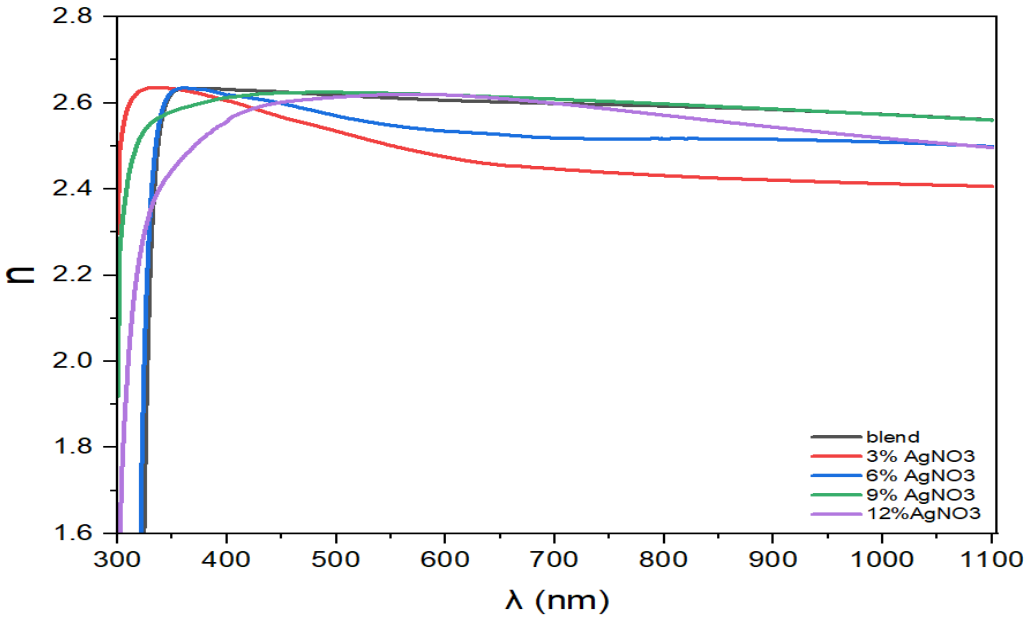

Figure 4: The correlation between refractive index and wavelength of light for PPy:PEO blend nanocomposites with varying concentrations of $AgNO_3$ (0, 3, 6, 9, and 12wt. %).

3.2. Electrical properties

- Hall Effect Measurement

The Hall coefficient (R_H), carrier type, charge carrier concentration (N_H), and hole transfer (μ_H) are assessed via Hall measurements performed at the Scientific Research Commission. Table 2 presents the variations in μ_H, N_H, and R_H with varying concentrations of $AgNO_3$ in PPy:PEO polymer blends to prepare nanocomposite films incorporating varying amounts of $AgNO_3$ NPs. The pure PPy:PEO blend film exhibits a negative Hall coefficient (R_H = -2.544 x 10^7 cm^3/C). This feature indicates that the majority charge carriers in an n-type semiconductor are electrons. While PPy is typically a p-type conducting polymer, the n-type behavior in the polymer blend could be attributed to specific synthesis conditions, the influence of the PEO matrix, or unintentional dedoping after polymer mixing. A significant change occurs when $AgNO_3$ is added. The Hall coefficient becomes positive for all concentrations. This n-type-to-p-type transition is a crucial finding. It confirms that holes have become the dominant charge carriers. This was because PPy acts as a reducing agent for Ag^+ ions, and in the process, the PPy chains become oxidized. This oxidation creates positive charge carriers (polarons and bipolarons) along the polymer blend backbone, which function as mobile holes [29, 30]. The carrier's concentration is calculated from the Hall coefficient using the Eq. (1), where e is the elementary charge [31].

$$N_H = \frac{1}{e\,|R_H|} \qquad (1)$$

The carrier concentration increases steadily with increasing $AgNO_3$ content, rising from 2.453 × 10^{11} cm^{-3} in the pure polymer blend to 6.810 × 10^{11} cm^{-3} at 12wt.% of $AgNO_3$. This increase directly correlates with the previously observed enhancement in electrical conductivity. The formation of Ag NPs via the oxidation of PPy inherently

generates more charge carriers (holes). Therefore, the primary reason for the enhanced conductivity is the significant increase in the population of available charge carriers [32].

Carrier mobility, a measure of how easily charge carriers move through the material, is calculated as Eq. (2), where σ is the DC conductivity [33]:

$$\mu_H = |R_H|\sigma \quad (2)$$

The mobility displays a more complex, non-monotonic behavior. It drops sharply at 3wt.% of $AgNO_3$, then progressively increases with concentration from 6 to 12 wt.%. The initial introduction of a small amount of Ag NPs (3wt.%) can induce structural disorder. These nanoparticles can act as scattering centers, impeding the movement of charge carriers until an effective conductive network forms. This increased scattering reduces mobility. As the Ag NP concentration increases from 6 to 12 wt.%, the particles become closer and begin to form an interconnected conductive network. This network provides "bridges" for charge carriers to hop between polymer chains more easily, reducing the energy barriers and increasing the mean free path. This improvement in the film's morphology and connectivity enhances charge-carrier mobility. The increase in mobility at higher concentrations, along with the increased carrier concentration, contributes to the overall rise in conductivity.

Table 2: The variation values of μ_H, N_H, and R_H with concentrations of $AgNO_3$ NPs in PPy:PEO polymer blend to prepare nanocomposite films.

PPy:PEO/ $AgNO_3$ wt.%	Type	μ_H (cm^2/v.sec)	N_H (cm^{-3})	R_H (cm^2/c)
0	n	2.551×10^2	2.453×10^{11}	-2.544×10^7
3	p	9.440×10^{-1}	1.170×10^{11}	5.334×10^7
6	p	3.910×10^2	5.040×10^{10}	1.239×10^8
9	p	2.990×10^2	6.062×10^{11}	1.030×10^7
12	p	8.453×10^2	6.810×10^{11}	9.166×10^6

- **D.C Electrical Conductivity ($\sigma_{d.c}$)**

Fig. 5 illustrates the variation in DC electrical conductivity ($\sigma_{d.c}$) for the PPy:PEO polymer blend films as a function of $AgNO_3$ concentration, measured at 65 °C. The conductivity initially increases significantly as the $AgNO_3$ concentration is increased from 0 to 9 wt.%. The value rises from approximately 1×10^{-6} $S \cdot cm^{-1}$ for the pure blend to a peak value of about 5.5×10^{-6} $S \cdot cm^{-1}$ at 9wt.% $AgNO_3$. After reaching this maximum value at 9 wt.% $AgNO_3$, the conductivity begins to decrease as the concentration is further increased to 12 wt. %, this behavior is characteristic of polymer nanocomposites, in which a conductive filler is dispersed within an insulating or semiconducting polymer matrix.

As discussed earlier in the absorption spectrum, the addition of $AgNO_3$ leads to the in-situ formation of highly conductive Ag NPs within the PPy: PEO matrix. PPy acts as a reducing agent for Ag^+ ions, creating metallic Ag NPs. When the concentration of Ag NPs increases, the average distance between them decreases. This facilitates the formation of a continuous network of conductive pathways throughout the polymer matrix. The Ag NPs serve as "conducting bridges" that help charge carriers (like polarons and bipolarons in PPy) move between the polymer chains. This procedure reduces the energy barrier for charge transport, thereby enhancing conductivity.

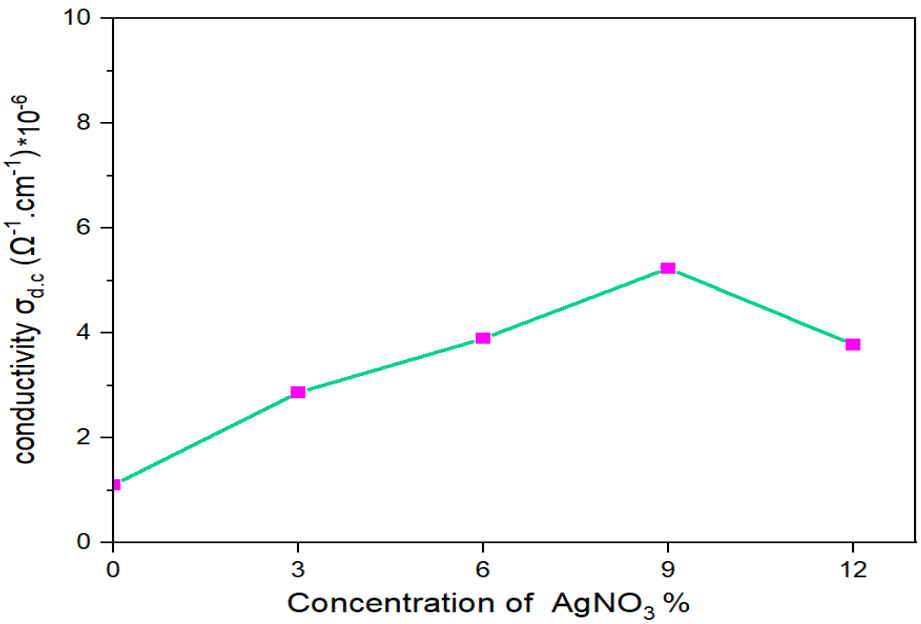

Figure 5: Variation in electrical conductivity ($\sigma_{d.c}$) at 65 °C with the concentration of $AgNO_3$ in the polymeric blend.

At higher concentrations (beyond the optimal 9 wt.%), Ag NPs tend to agglomerate or form large clusters due to their high surface energy. Instead of forming a fine, well-distributed network, they form large, isolated aggregates. These large agglomerates can act as "scattering centers" or "traps" for charge carriers, hindering their mobility. They disrupt the continuity of the conductive network that was formed at lower concentrations, effectively increasing the material's resistance and decreasing its conductivity. Paradoxically, the formation of large clusters can increase the effective distance that charge carriers must travel between clusters, making charge hopping less efficient compared to a well-dispersed network of smaller particles [34].

- **A.C Electrical Conductivity ($\sigma_{a.c}$)**

Fig. 6 displays the relationship between the logarithm of AC conductivity (Ln σ) and the logarithm of angular frequency (Ln ω) for the PPy:PEO polymer blend and its nanocomposite films doped with different concentrations of $AgNO_3$ (3, 6, 9, and 12wt.%). This type of plot is crucial for understanding charge-transport mechanisms in the material. The graph clearly shows that for all the films (both the pure polymer blend and the ones with added $AgNO_3$), the AC conductivity ($\sigma_{a.c}$) goes up as the frequency goes up. This behaviour is a characteristic feature of disordered and amorphous materials, including conductive polymers.

The conductivity behavior across the frequency spectrum can be divided into two main regions: first, the low-frequency region (Plateau Region). At lower frequencies, the conductivity is nearly independent of frequency and approaches the DC conductivity. This conductivity is due to the long-range movement of charge carriers through the material's established percolation paths. Second, High-Frequency Region (Dispersion Region): In this region, the conductivity shows a strong, near-linear dependence on frequency. This behavior was due to short-range, localized charge carrier motion, such as hopping between adjacent localized sites. At high frequencies, the electric field changes rapidly, enabling charge carriers to hop between nearby sites, thereby contributing significantly to the overall conductivity [35].

It is evident from the graph in Fig. 6 that the overall AC conductivity at any given frequency increases with the addition of $AgNO_3$, with the highest conductivity values observed for the 9 and 12 wt.% concentrations. This observation is in excellent agreement with the previous DC conductivity and Hall effect results. The incorporation of Ag NPs enhances conductivity by increasing the carrier concentration, providing more charge carriers to participate in conduction at all frequencies.

Also, the Ag NPs create pathways that help move charges over long distances (which boosts $\sigma_{d.c}$) and allow charges to jump between the polymer blend chains and nanoparticles over shorter distances (which increases the frequency-dependent conductivity). The higher amounts (9 and 12 wt.%) exhibit the best conductivity because they have a more extensive and interconnected network of Ag NPs, which improves both types of charge transport.

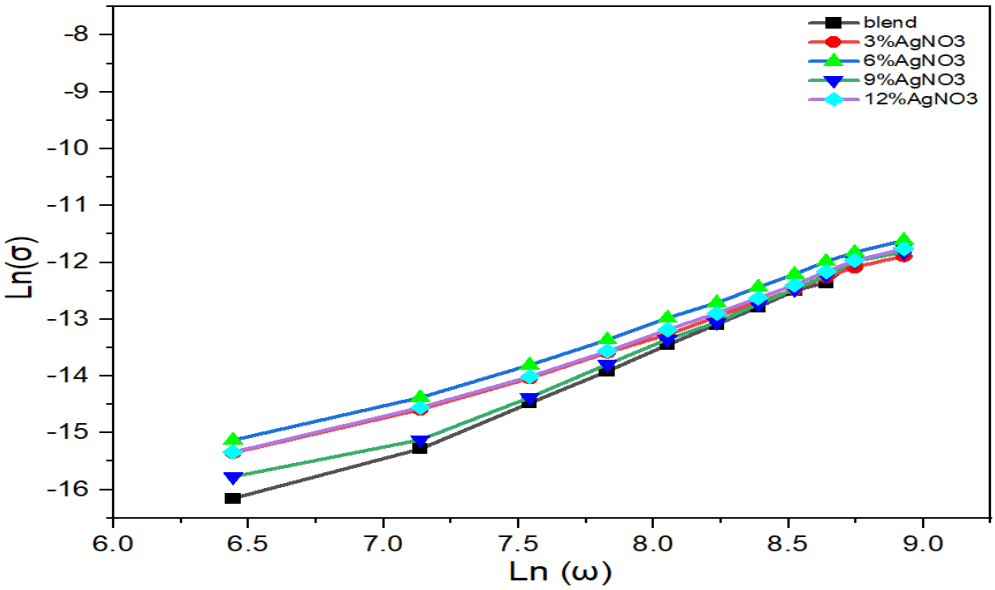

Figure 6: The relation between Ln (ω) and Ln(σ) for polymeric nanocomposites (PPy:PEO) after doping with different concentrations of $AgNO_3$.

4. Conclusions

The results of this study demonstrate that incorporating a PPy/PEO blend with oxidized $AgNO_3$ nanoparticles significantly affects both their optical and electrical properties. In terms of optical behavior, the UV-Vis spectra showed a clear absorption peak around 400 nm, with its intensity enhancing as the dopant concentration increased, reflecting improved optical responsiveness. A noticeable transition in charge carrier type was observed from n-type to p-type as the concentration of $AgNO_3$ increased, indicating a shift in the conduction mechanism within the material. Electrical measurements revealed that the DC resistance decreased with rising temperature, confirming semiconductor-like behavior, while the AC conductivity increased notably at higher frequencies. Overall, these findings suggest that incorporating $AgNO_3$ nanoparticles into polymer matrices offers a practical and efficient approach to tailor and enhance the functional properties of conductive polymer films. This opens promising possibilities for their application in advanced electronic devices, sensors, and optoelectronic systems.

Conflict of Interest

Authors declare that they have no conflict of interest.

References

1. N. Qureshi, V. Dhand, S. Subhani, R. S. Kumar, N. Raghavan, S. Kim, and J. Doh, Adv. Mater. Technol. **9**, 2400250 (2024). https://doi.org/10.1002/admt.202400250.
2. B. M. Abed and M. G. Hammed, Iraqi J. Appl. Phys. **21**, 408 (2025).
3. M. Bustamante-Torres, D. Romero-Fierro, B. Arcentales-Vera, S. Pardo, and E. Bucio, Polymers. **13**, 2998 (2021). https://doi.org/10.3390/polym13172998.
4. R. A. Omar and M. G. Hammed, J. Inorg. Organomet, Polym. Mater. **35**, 3158 (2025). https://doi.org/10.1007/s10904-024-03450-4.
5. D. Kincal, A. Kumar, A. D. Child, and J. R. Reynolds, Synth. Met. **92**(1), 53 (1998). https://doi.org/10.1016/S0379-6779(98)80022-2.
6. N.T. Kemp, G.U. Fianagan, A.B. Kaiser, H.J. Trodahl, B. Chapman, A.C. Partridge, and R.G.Buckle, Synth. Met. **101**, 434 (1999). https://doi.org/10.1016/S0379-6779(98)01118-7.
7. K. Namsheer and C. S. Rout, RSC Adv. **11**, 5659 (2021). https://doi.org/10.1039/D0RA07800J.
8. A.-U. D. Sabah, I. M. Ibrahim, and M. G. Hammed, Ionics, **31**, 9815 (2025). https://doi.org/10.1007/s11581-025-06488-7.
9. Q. M. Jebur, A. Hashim, and M. A. Habeeb, Trans. Electr. Electron. Mater. **20**, 334 (2019). https://doi.org/10.1007/s42341-019-00121-x.
10. G. Gelardi, S. Mantellato, D. Marchon, M. Palacios, A. Eberhardt, and R. Flatt, *Science and Technology of Concrete Admixtures*, Elsevier, 149 (2016). https://doi.org/10.1016/B978-0-08-100693-1.00009-6.
11. M. Dalton, F. Ebrahimi, H. Xu, K. Gong, G. Fehrenbach, E. Fuenmayor, EJ Murphy, and I. Major, Macromol. **3**, 431 (2023). https://doi.org/10.3390/macromol3030026.
12. K.K. Ahmed, D.Q. Muheddin, P. A. Mohammed, G. S. Ezat, A. R. Murad, B. Y. Ahmed, S. A. Hussen, T. Y. Ahmed, S. M. Hamad, O. Gh. Abdullah, and S. B. Aziz, Results Phys. **56**, 107239 (2024). https://doi.org/10.1016/j.rinp.2023.107239.
13. A. Dube, S. J. Malode, A. N. Alodhayb , K. Mondal , N.P. Shetti, Sci. **103**, 1931 (2024). https://doi.org/10.1016/j.talo.2024.100395.
14. A. A. Khudhair, S. N. Mazhir, and M. G. Hammed, Plasmonics, **20**, 7195 (2025). https://doi.org/10.1007/s11468-024-02622-9.
15. H.A. Saleh, H.A. Younis. Egypt. J. Chem. **65**, 1, 199 (2022). http://ejchem.journals.ekb.eg/.
16. H. Ali , S. Ali , K. Ali , S. Ullah , P.M. Ismail , M. Humayun , Ch. Zeng, Results in Engineering, **27**, 106151 (2025). https://doi.org/10.1016/j.rineng.2025.106151.
17. H. Y. Mohammed, M. A. Farea, M. H. Albuhairi, and M. D. Shirsat, *Synthetic Metals,* **302**,117546 (2024). https://doi.org/10.1016/j.synthmet.2024.117546.
18. D. Essam, A. M. Ahmed, A. A. Abdel-Khaliek, M. Shaban, and M. Rabia, *Scientific Reports,* **15**, 2698 (2025). https://doi.org/10.1038/s41598-024-84848-5.
19. E. Abdelrazek, A. Abdelghany, S. Badr, and M. Morsi, Res. J. Pharm. Biol. Chem. Sci. **7**, 1877 (2016). https://doi.org/10.1016/j.jmrt.2017.06.009.
20. H. J. Jang, B.J. Shin, E.Y. Jung, G.T. Bae, J.Y. Kim and H.S.Tae, Applied Surface Science, **608**, 155129 (2023). https://doi.org/10.1016/j.apsusc.2022.155129.
21. W.J. Ho, J.C. Chen, J.J. Liu, and C.H. Ho, Appl. Surf. Sci. **532**, 147434 (2020). https://doi.org/10.1016/j.apsusc.2020.147434.
22. W. Dwandaru, A. Fathia, and R. Wisnuwjaya, J. Phys.: Conf. Ser. **1097**, 012011 (2018). https://doi.org/10.1088/1742-6596/1097/1/012011.
23. V. J. Jalal, J. Phys. Commun. **8**, 055004 (2024). https://doi.org/10.1088/2399-6528/ad3c5f.
24. A. S. Hussein, M. H. Shinen, and M. S. Abdali, J. Univ. Babylon Pure Appl. Sci. **27**, 169 (2019).
25. H. E. Ali, H. S. M. Abd- Rabboh, N. S. Awwad, H. Algarni, M. A. Sayed, A. F. A. El- Rehim, M. M. Abdel-Aziz, and Y. Khairy, Optik **247**, 167863 (2021). https://doi.org/10.1016/j.ijleo.2021.167863.
26. M. Fox, *Optical Properties of Solids*, (Oxford University press, New York) 2nd edition, (2010).
27. D. Debnath and S. K. Ghosh, ACS Applied Nano Materials **5**, 1621 (2022). https://doi.org/10.1021/acsanm.1c04393.
28. M. Abdelaziz and E. Abdelrazek, J. Electron. Mater. **42**, 2743 (2013). https://doi.org/10.1007/s11664-013-2742-8.
29. D. T. Scholes, S. A Hawks, P.Y Yee, H. Wu, J.R Lindemuth, S.H Tolbert, and B.J Schwartz, J. Phys. Chem. Lett. **6**, 4786 (2015). https://doi.org/10.1021/acs.jpclett.5b02310.
30. A. Bahrami, Z. A. Talib, W. M. M. Yunus, K. Behzad, M. M. Abdi, and F. U. Din, Int. J. Mol. Sci. **13**, 14917 (2012). https://doi.org/10.3390/ijms131114917.
31. R. S. Popovic, *Hall Effect Devices* (CRC Press) 2nd edition**,** (2003).
32. D. Nerkar, S. Panse, S. Patil, S. Jaware, and G. Padhye, Sens. Transducers. **202**, 76 (2016).

33. M. M. Sundaram and A. Pivrikas. Coatings. **13**, 1657 (2023). https://doi.org/10.3390/coatings13091657.
34. S. S. Rao, K. S. Rao, M. Shareefuddin, U. S. Rao, and S. Chandra, Solid State Ionics **67**, 331 (1994). https://doi.org/10.1016/0167-2738(94)90220-8.
35. F. M. H. AlSulami, A. I. Al-Sulami, A. Rajeh, J. Alnawmasi, E. M. Abdelrazek, M. O. Farea, R H. Aldahiri, and H. M. Alghamdi. Opt. Mater. **152**, 115515 (2024). https://doi.org/10.1016/j.optmat.2024.115515.

تحضير وتوصيف مزيج PPy:PEO المشوب بجسيمات $AgNO_3$ النانوية: دراسة بصرية وكهربائية

مروان ماجد فاضل[1] و محمد غازي حمد[1]

[1]قسم الفيزياء، كلية العلوم، جامعة الانبار، الانبار، العراق

الخلاصة

تم تصنيع أغشية نانوية مركبة، مصنوعة من البولي بيرول (PPy) وأكسيد البولي إيثيلين (PEO)، قابلة للتطعيم بجزيئات نانوية من نترات الفضة ($AgNO_3$)، باستخدام تقنية الرش الحراري عند درجة حرارة الغرفة. أُجريت دراسة منهجية للخواص البصرية والكهربائية للأغشية المُحضّرة، وذلك تبعًا لتركيز المُطعِّم (0، 3، 6، 9، و12% وزنيًا). يُظهر مطياف الأشعة فوق البنفسجية والمرئية ذروة امتصاص ملحوظة عند حوالي 400 نانومتر. وتؤدي التركيزات العالية من نترات الفضة إلى زيادة شدة هذه الذروة، خاصةً في العينة التي تحتوي على 12% من نترات الفضة. استُخدمت قياسات هول لتحديد نوع وتركيز حاملات الشحنة، بالإضافة إلى قياس حركة هول (ميكروهنري). أظهرت النتائج أن الأغشية النانوية المركبة كانت ذات معامل هول سالب (من النوع n) قبل إضافة جزيئات نترات الفضة النانوية. بينما أظهرت أغشية مزيج البوليمرات موصلية من النوع p مع معامل هول موجب عند جميع تركيزات جزيئات نترات الفضة النانوية. في دراسات التيار المستمر، تنخفض المقاومة الكهربائية مع ارتفاع درجة الحرارة، بينما ترتفع موصلية التيار المستمر لغشاء النانو المركب مع ارتفاع تركيز جسيمات نترات الفضة النانوية. في جميع العينات المنتجة، تزداد الموصلية الكهربائية المتناوبة مع زيادة التردد. عند الترددات المنخفضة، لا تتغير الموصلية الكهربائية المتناوبة ($\sigma_{a.c}$).

الكلمات المفتاحية: نترات الفضة النانوية، خليط البولي بايرول:بولي اثلين أوكسيد، الخصائص البصرية، تأثير هول، التوصيلية الكهربائية.